Chapter 2

Preparation of (1-x)BNT-xBaT and (1-X)[0.90BNT-0.10PT]-xBaT Solid Solutions

2.1. Introduction

$Bi_{1/2}Na_{1/2}TiO_3$ (BNT), a ferroelectric at room temperature has the perovskite structure with a general formula $A^{XII}\ B^{VI}\ O_3{}^{VI}$ in which A and B are cations at the different sites, A site and B site respectively. The Roman numbers represent the cation:anion coordination number. Two types of cations, Bi and Na are in the A site and Ti is in B site.

In the past, researchers prepared ceramic specimens of BNT by a conventional technique. Pure grades or reagent grades of mixed oxides (15), Bi_2O_3, Na_2CO_3, TiO_2 were weighed in a stoichiometric ratio and then milled. The milled powder was calcined at 750-800 °C for one hour. The calcined powder was ground and pressed into disks and then sintered at 1080-1100 °C for two hours (15). It was found that the density was up to 95% of the theoretical density. The weight loss, however, was not reported and the dielectric constant was extremely low at room temperature, 244 (15). In general, the best dispersion of particles are obtained by milling in a liquid medium, water or alcohol. However, for the electronic material, water may react with the active centers created by the grinding action and reduce the reactivity. Two means of preparation of BNT-PT solid solution were compared by Isupov et al (20). The first one is preparation of BNT-PT soild solution directly from oxides and carbonates and the other, he prepared the perovskite at first and combined the synthesized titanates. In the preparation directly from oxides and carbonates, all raw materials were mixed dry in a

ball mill, following by calcining at 850 °C for three hours. In the second, $Bi_{1/2}Na_{1/2}TiO_3$ (BNT) and $PbTiO_3$ (PT) were prepared separately. Then, these two titanate compounds were dry mixed in the ball mill for 4 hours, calcined and ground. When pressed to disks, the powder from those two methods were sintered in air at 1180-1200 °C for 20-30 minutes in a furnace. The loss of lead reported was increased considerably and commensurately with increasing the concentration of $PbTiO_3$ of up to 90%. such that there should be a sintering in closed capsules if a composition contained lead oxide. However, the reported dielectric properties of samples with or without lead loss were of similarity, regardless of the method of preparation. Their dielectric constant at room temperature decreased as the concentration of Pb increased.

2.2. Preparation

All compositions for this research were prepared by mixing and calcining all oxides and carbonates. These compositions studied in these systems were

2.2.1. (1-x)BNT-x$BaTiO_3$ or (1-x)BNT-xBaT

(a). BNT ; x= 0

(b). 0.95BNT-0.05BaT ; x= 0.05

(c). 0.90BNT-0.10BaT ; x= 0.10

(d). 0.85BNT-0.15BaT ; x= 0.15

2.2.2 (1-x)[0.90BNT-0.10PT]-x$BaTiO_3$ or (1-x)[0.90BNT-0.10PT]-xBaT

(a). 0.90BNT-0.10PT ; x= 0

(b). 0.95(0.90BNT-0.10PT)-0.05BaT ; x= 0.05

(c). 0.90(0.90BNT-0.10PT)-0.10BaT ; x= 0.10

(d). 0.85(0.90BNT-0.10PT)-0.15BaT ; x= 0.15

Starting raw materials were Bi_2O_3, Na_2CO_3, TiO_2, PbO and $BaCO_3$, as listed in Appendix A. They were weighed according to stoichiometry and mixed by wet ball-milling with ZrO_2 grinding media and ethyl alcohol as a solvent in a high density polyethylene bottle for 6-8 hours. After drying, the mixture was calcined with a heating rate of 2 °C /min., and soaked for 2 hours at 850 °C in oxygen. The calcined materials were milled and 2% weight of polyvinyl alcohol were added in the last hour of milling. The powders were pressed into disks of 13 mm diameter by a single action dry-press with a pressure of 82 MPa.

After burning-out binder with a heating rate of 1 °C /min and holding at 550 °C in oxygen, the disks were weighed before firing to determine the weight loss. Then the disks were placed on Pt-foil in a closed crucible and sintered with a heating rate of 4 °C /min and an hour soaking period at the sintering temperature. The sintered samples were cooled in the furnaces.

2.3. Reaction Analysis Before and After Calcination of Powder

Studied from Takenaka's work (17), powder of $(Ba_{1/2}Na_{1/2})TiO_3$ -$BaTiO_3$ solid solution was calcined at 800 °C for one hour. In contrast, the powder of this experiment was calcined at 850 °C for two hours since a reaction was not complete at 800 °C observed from DTA (differential thermal analysis), as shown in Fig.1. The amount of heat exchange and the temperature at which the reactions occurred can be characterized from DTA The evident "fingerprint" of a material is influenced by reactions results in

heat absorption(endothermic) or heat evolution(exothermic) (21). As shown in Fig.1, the endothermic reaction starts around 100 °C and finishes about 830 °C. The area of DTA curve (or peak) is directly proportional to the enthalpy change and indirectly proportional to the heat change (21) involved. This technique can be used for semiquantitative and in some cases, quantitative analysis. After calcining, the powder was characterized by DTA to investigate the remaining reactions. There is no peak appeared on Fig.2 indicating complete reaction after calcining at 850 °C. Therefore, the calcining temperature at 850 °C is used through this research.

In Kuharuangrong's works (6,7,19), powder of 0.90BNT-0.10PT solid solution was calcined at 750 °C and 800 °C for Takenaka's work (18). Therefore, in this experiment the powder of 0.90BNT-0.10PT composition is calcined at 750 °C and its DTA data shows a complete reaction before 750 °C as illustrated in Fig.2. However, Ba doped 0.90BNT-0.10PT system undergoes the reaction above 750 °C as shown in Fig.2 indicating that the reaction is over around 850 °C higher than undoped system due to high sintering temperature of $BaTiO_3$

The results from TGA (thermogravimetric analysis) indicate that there is a weight loss of the system, as shown in Table.2. TGA measures the mass of the test sample as a function of the temperature. The resulting mass change versus temperature curve provides useful information regarding the study of reaction process. Most of the weihgt losses come from CO_3^{2-} in raw materials changed into CO_2. The TGA curves as shown in Fig.3-4 and Table.2 show the expected results. That is, 5% Ba doped BNT gives the weight loss more than undoped material. However, a measured weight loss from TGA is higher than a calculated weight loss. It may be other raw materials having a high volatility such as Bi_2O_3 and Na_2CO_3 that loss from

the solid solutions. For 5% Ba doped BNT, the difference between TGA measurement and calculation is greater than BNT although the quantities of Bi_2O_3 and Na_2CO_3 are smaller. The reason should that the calcining temperature of 5% Ba doped BNT (850 ^oC) is more than that of BNT (750 ^oC). In addition, PbO affects strongly the weight loss, for example in Fig.3 and Fig.5, carbonate compound of both systems is only Na_2CO_3 . Thus, the weight loss should depend on merely Na_2CO_3 but Fig.5 shows that it relies on PbO due to a higher weight loss.

Table 2. Comparison of weight loss from the calculation and the TGA measurement excluding moisture content.

Compositions	% Weight loss from measurement	% Weight loss from calculation	Differences
BNT	5.1	4.9	0.2
BNT-5BaT	7.5	5.6	1.9
BNT-10BaT	6.3	4.3	2.0

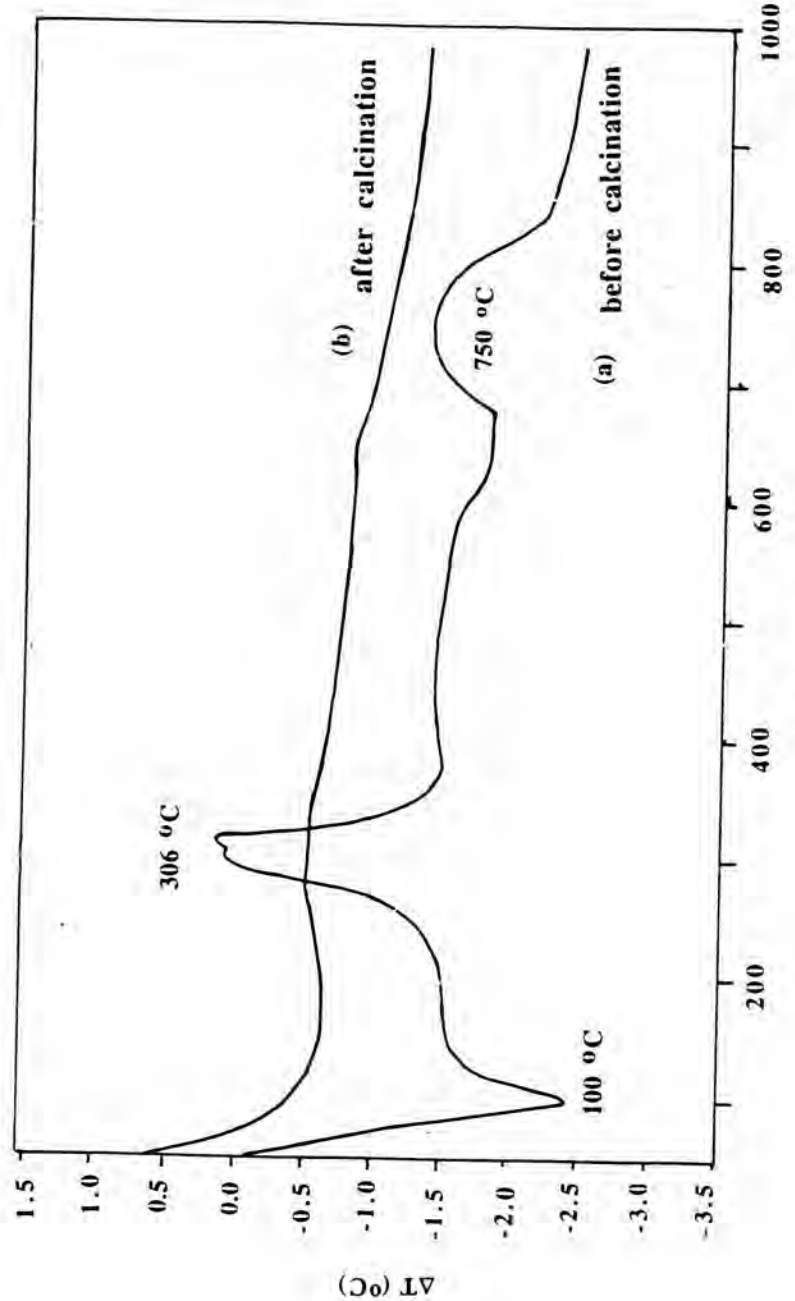

Fig.1 DTA curves of 0.95BNT-0.05BaT before and after calcination
(a) before calcination (b) after calcination

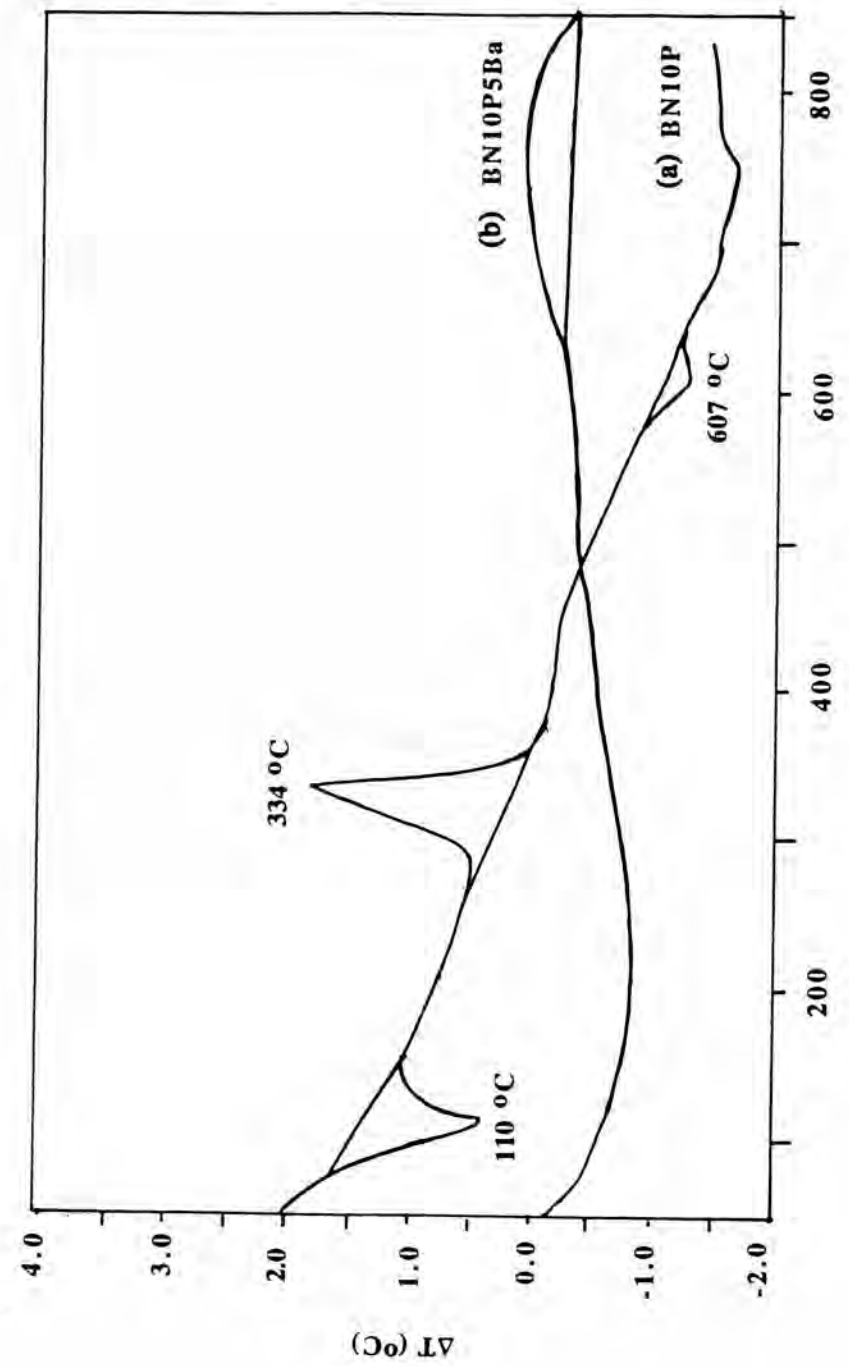

Fig.2 DTA curves of 0.90BNT–0.10PT before calcination and (0.90BNT–0.10PT)–0.15BaT after calcination (a) 0.90BNT–0.10PT(BNT10P) (b) 0.85(0.90BNT–0.10PT)–0.15BaT(BN10P 5Ba)

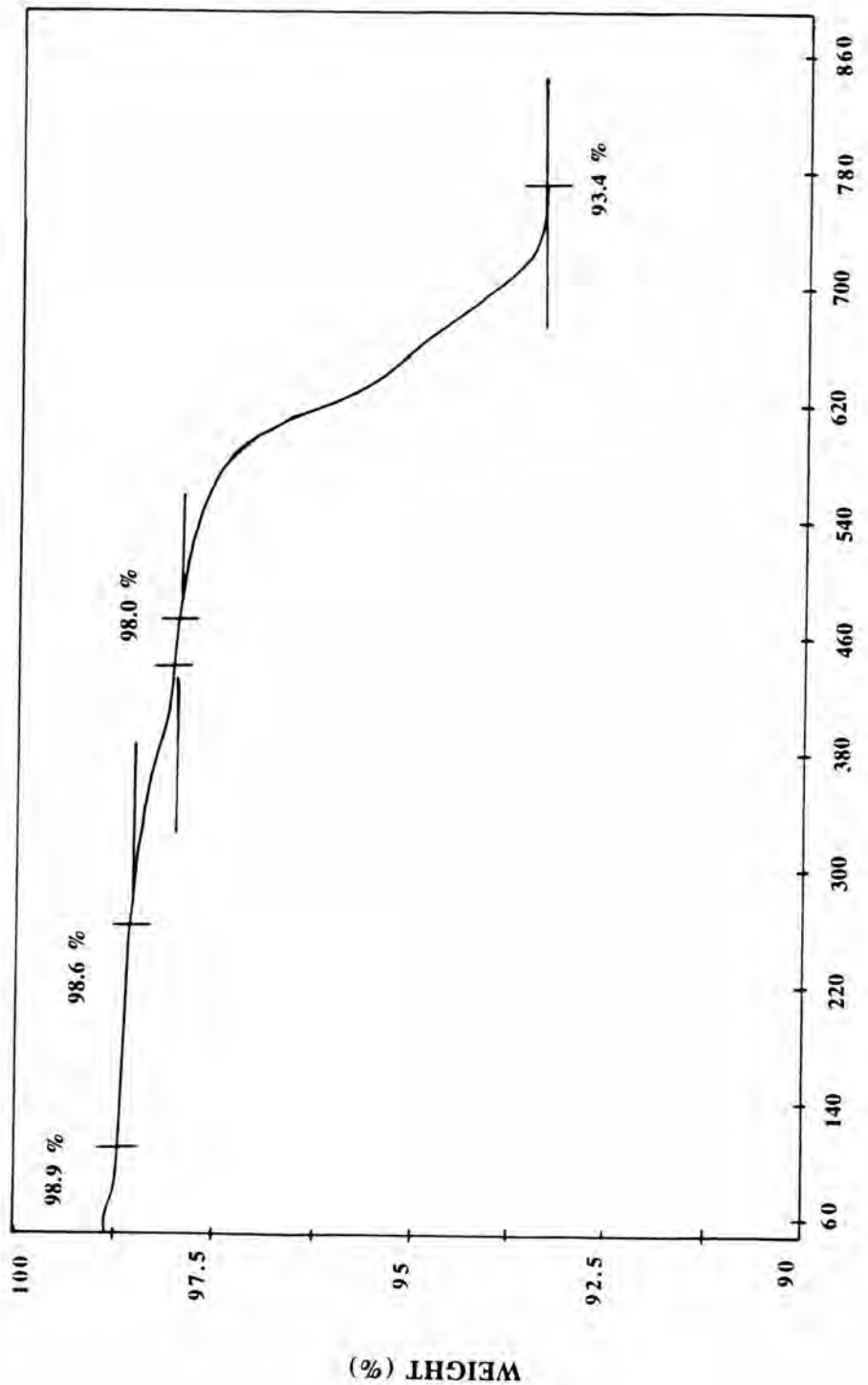

Fig.3 TGA curve of BNT

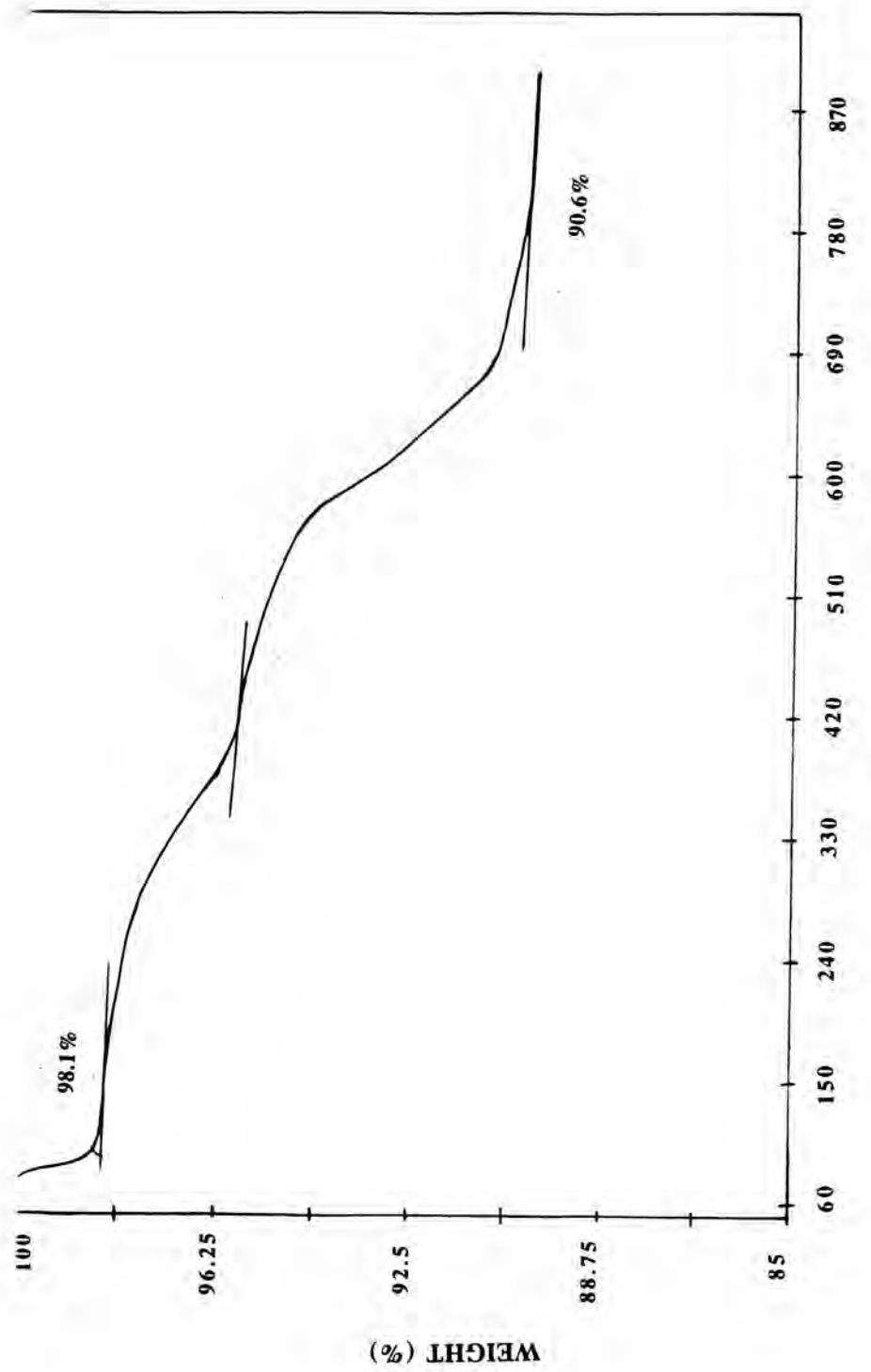

Fig.4 TGA curve of 0.95BNT–0.05BaT

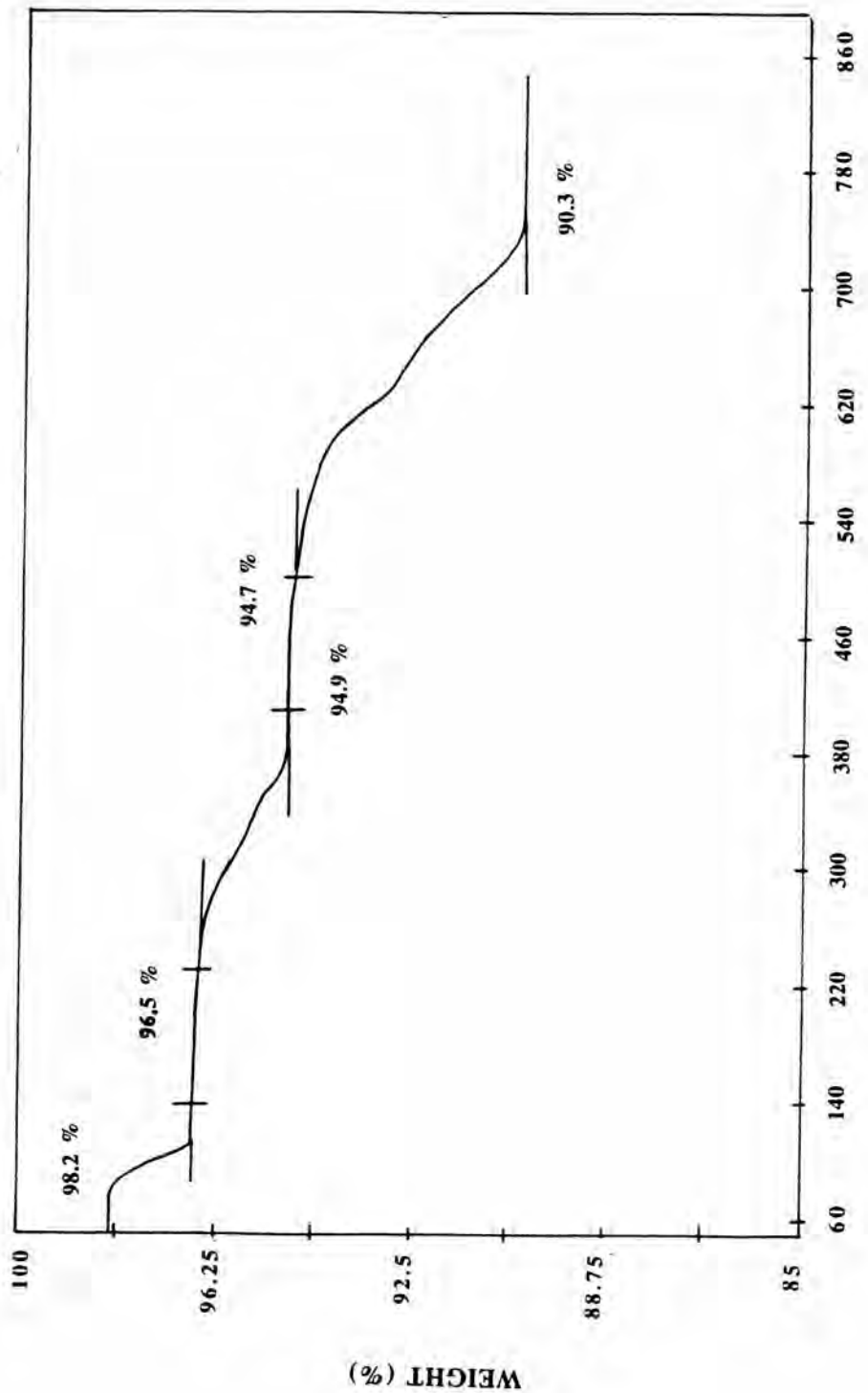

Fig.5 TGA curve of 0.90BNT-0.10PT

2.4. Weight loss, Shrinkage and Microstructure after Sintering

The weight loss was determined from the weight before and after sintering.

The firing shrinkage was determined from the diameter of samples before and after sintering.

The microstructure of the samples was observed from the JEOL JSM-5140 LV Scanning Electron Microscope (SEM). The samples were polished and thermally etched at 100 °C below the sintering temperature. The second phases were detected from the JEOL JSM-6400 Energy Dispersive Spectroscopy (EDS) and Wavelength Dispersive Spectroscopy (WDS).

2.5. Results and Discussion

The results of the weight loss and shrinkage as functions of firing temperature and compositions are shown in Table 3 and 4.

Table 3. Weight loss and shrinkage versus temperatures and compositions in $(1-x)Bi_{1/2}Na_{1/2}TiO_3-xBaTiO_3$

$Bi_{1/2}Na_{1/2}TiO_3$

Firing temperature (°C)	% weight loss	% shrinkage
1150	-	-
1175	0.6	18
1200	0.7	18

$0.95Bi_{1/2}Na_{1/2}TiO_3$ - 0.05 $BaTiO_3$

Firing temperature (°C)	% weight loss	% shrinkage
1150	0.4	19
1175	0.6	19
1200	0.6	19

$0.90Bi_{1/2}Na_{1/2}TiO_3$ - 0.10$BaTiO_3$

Firing temperature (°C)	% weight loss	% shrinkage
1150	0.4	19
1175	0.5	18
1200	0.6	19

$0.85Bi_{1/2}Na_{1/2}TiO_3$ - 0.15$BaTiO_3$

Firing temperature (°C)	% weight loss	% shrinkage
1150	0.3	19
1175	0.4	19
1200	0.5	18

Table 4. Weight loss, shrinkage versus temperatures and compositions in $(1-x)[0.90\ Bi_{1/2}Na_{1/2}TiO_3 - 0.10\ PbTiO_3]-xBaTiO_3$

$0.90\ Bi_{1/2}Na_{1/2}TiO_3 - 0.10\ PbTiO_3$

Firing temperature (°C)	% weight loss	% shrinkage
1150	-	-
1175	0.5	19
1200	0.7	18

$0.95\ [0.90\ Bi_{1/2}Na_{1/2}TiO_3 - 0.10\ PbTiO_3]-0.05\ BaTiO_3$

Firing temperature (°C)	% weight loss	% shrinkage
1150	0.5	18
1175	0.6	18
1200	0.8	18

$0.90\ [0.90\ Bi_{1/2}Na_{1/2}TiO_3 - 0.10\ PbTiO_3]-0.10BaTiO_3$

Firing temperature (°C)	% weight loss	% shrinkage
1150	0.5	19
1175	0.7	18
1200	0.7	18

$0.85\ [0.90\ Bi_{1/2}Na_{1/2}TiO_3 - 0.10\ PbTiO_3]-0.15BaTiO_3$

Firing temperature (°C)	% weight loss	% shrinkage
1150	0.6	19
1175	0.6	18
1200	-	18

The shrinkage values are approximately 18-19%, as shown in Tables 3 and 4. There are no different results from both systems. It is showed that the range of sintering temperature between 1150-1200 °C does not affect the shrinkage. The results are reported that the trend of % weight loss increases as sintering temperature increases, which are partly different from Kuharuangrong's work (6). In addition, as a function of an amount of %Ba doped BNT, it is found that the weight loss decreases with the increase of %Ba doped BNT due to the decrease of high volatility compound, Bi_2O_3 and Na_2CO_3. For Ba doped 0.90BNT-0.10PT, the value of weight loss is more than that of Ba doped BNT but it is likely constant as %Ba increased. For Ba doped BNT, the weight loss comes from Bi and Na volatility and Pb also results in the weight loss for Ba doped 0.90BNT-0.10PT as compared with Pb-free-system has less the weight loss. However, most of the weight loss of both solid solutions are less than 0.9% which is similar to Kuharuangrong's work (6). In order to control PbO volatility and attain higher dielectric constant, sintering in a closed crucible is employed for all samples during preparation in this work.

The results of microstructure from SEM indicate that grain size of both solid solution systems are similar. That is, as %Ba dopant increases the grain size decreases as shown in Fig.10-14. It can be suggested that the addition of Ba in both BNT and 0.90BNT-0.10PT inhibited grain growth resulting from grain boundary motion. Ba can dissolves in crystal lattice and exists around grain boundaries to restrict their motion. In addition, there is an insignificant change in grain size of these systems with a futher increase of Ba content up to 15%. However, as a function of temperature as shown in Fig.6-9, the grain size increases when sintering temperature increases due to grain boundary motion. In comparison, grain size of Ba doped 0.90BNT-0.10PT as a function of sintering temperature is greater than that of Ba doped

BNT, as considered from Fig.7 (a) & (b) and Fig 9 (a) & (b). It is suspected that Ba can be more present at the grain boundary of BNT than 0.90BNT–0.10PT and play a part on suppressing grain boundary motion which causes the grain growth. It can be said that it can controll grain growth of BNT than that of 0.90BNT-0.10PT do. As compared with the grain size of 5% Ba doped BNT at the same sintering temperature, that of 5% Ba doped 0.90BNT-0.10PT is larger.

From the results of SEM photomicrographs, there are second phases existing in many samples. These second phases are observed from EDS. It is found that most of compositions consist of the second phases. Their shapes are different. As %Ba increases an quantity of second phase increases. 15% Ba doped BNT shows a more second phase in different shapes. One is circular and other is plate-like shapes. However, most of the second phases are Ba and Ti in almost equality, as depicted in Fig.15(a) and (b). From EDS, the second phase peaks consisting of Ba and Ti occur about 4.5-5.0 keV and show an overlapping of Ba and Ti peaks. To ensure the formation of both Ba and Ti, WDS is used to investigate these peaks. It is assured that there are both Ba and Ti occurring around 2.5 A°, as illustrated in Fig.18. The EDS-result of single-grains or matrix of 15% Ba doped BNT is shown in Fig.16. There are Na,Bi,Ti and Ba. This result assures that Ba can get in the grain boundary in the form of solid solution. In relavance to the result of the grain size of this system, Ba in second phases can no longer get in the grain boundary as %Ba is more than 10% such that the grain size does not increase significantly as %Ba increases. It can be said that there are Ba content excess in the reactions so Ba excess can not play a role to reduce grain size any more.

In Ba doped 0.90BNT-0.10PT system, it also has a more second phase existing in 10% Ba doped this system than 5%Ba dopant. There are two types of the second phase in 10% Ba. One is plate-like shape and other is short bar shape. Like Ba doped BNT systems, the components of the second phase in this samples are Ba and Ti, as shown in Fig.17.

The followings are SEM photomicrographs of the samples as a function of firing temperature, as shown in Fig. 6-9. and as a function of %Ba dopant, as shown in Fig. 10-14.

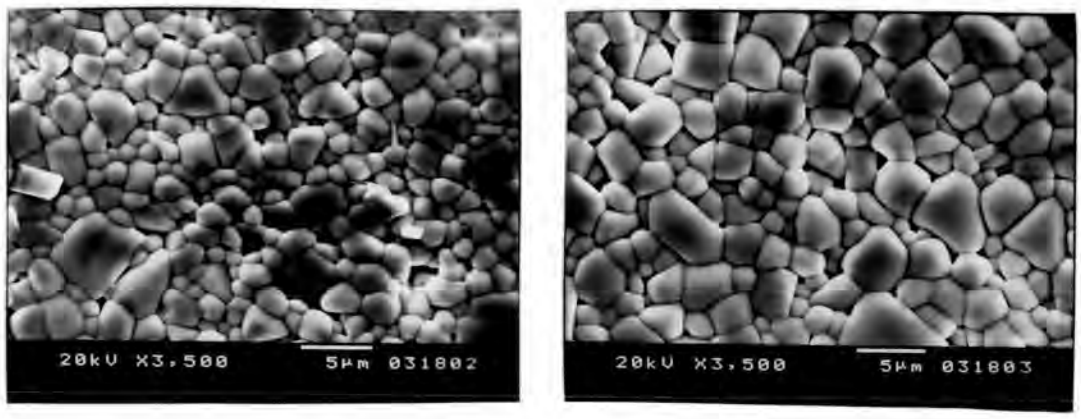

(a) (b)

Fig.6 SEM photomicrographs of BNT at different sintering temperatures
(a) 1175 °C (b) 1200 °C

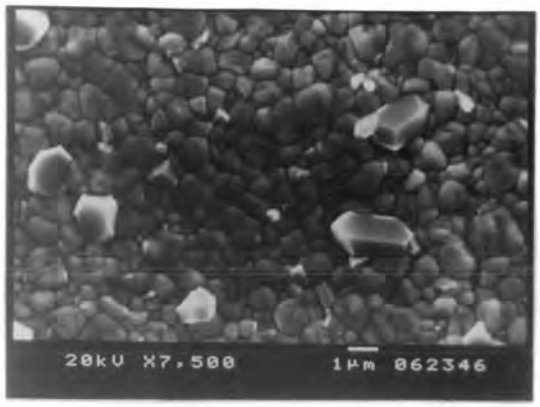

(a)

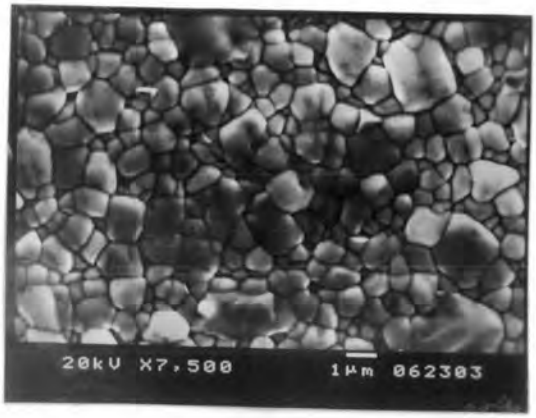

(b)

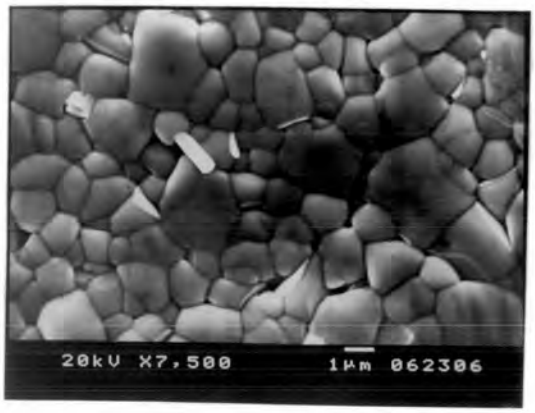

(c)

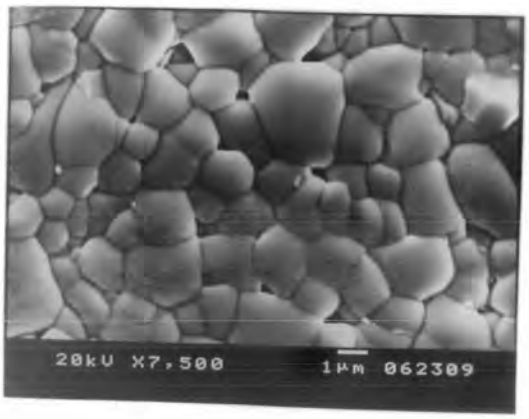

(d)

Fig.7 SEM photomicrographs of 0.95BNT–0.05BaT at different sintering temperatures (a) 1150 °C (b) 1175 °C (c) 1200 °C (d) 1225 °C

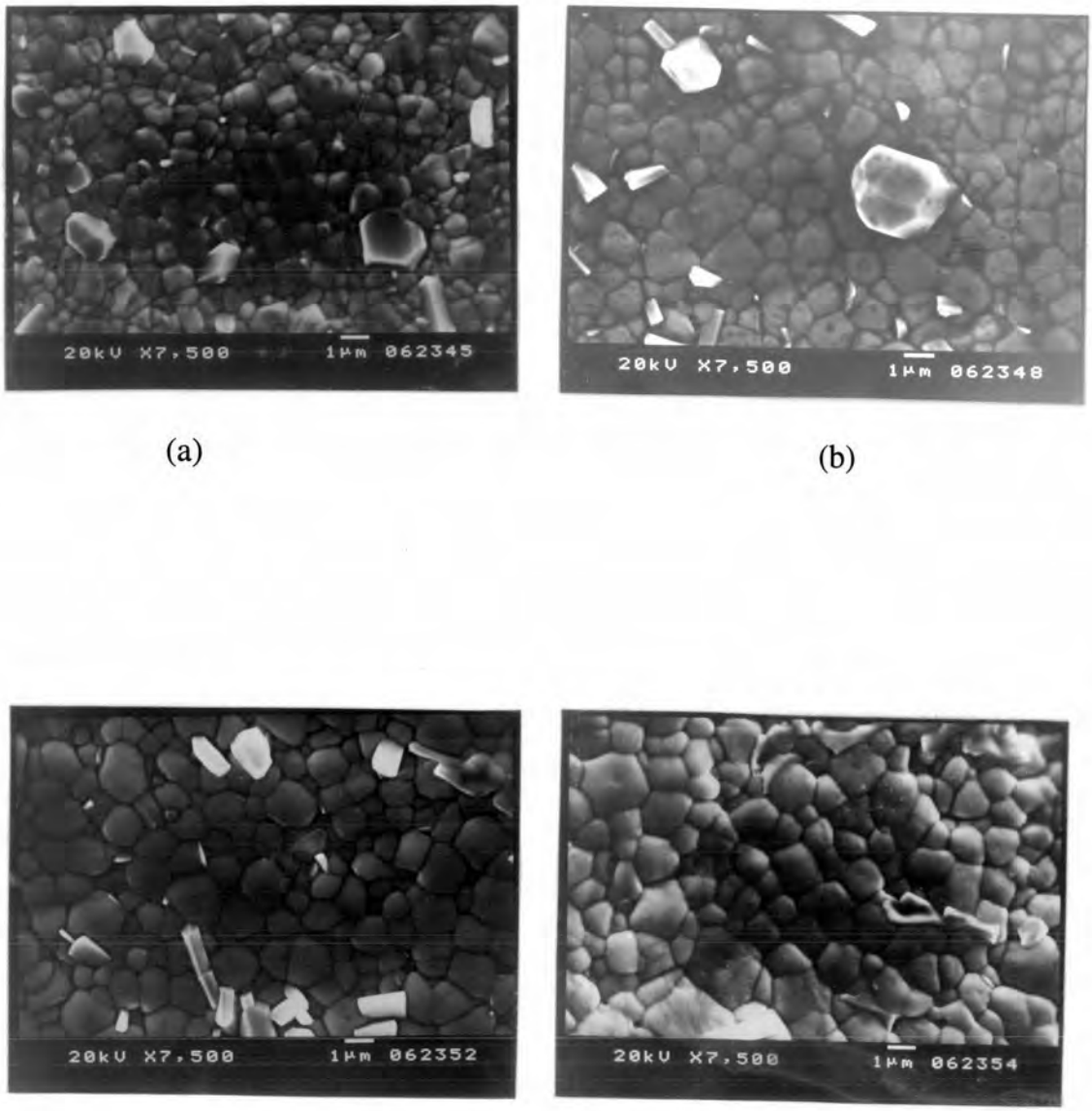

Fig.8 SEM photomicrographs of 0.90BNT-0.10BaT at different sintering temperatures (a) 1150 °C (b) 1175 °C (c) 1200 °C (d) 1225 °C

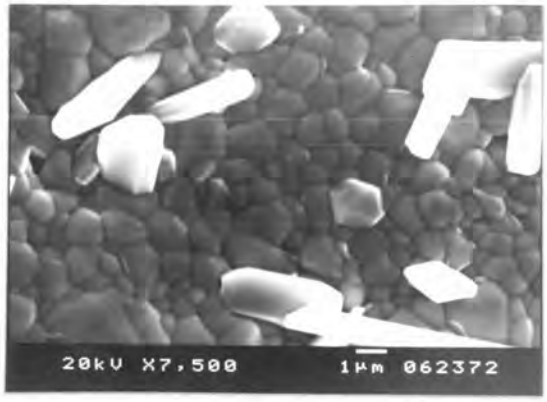

(a)

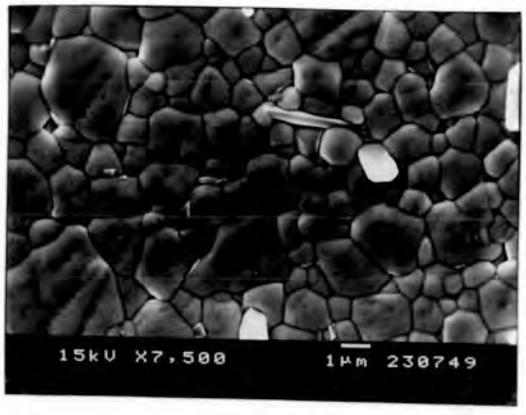

(b)

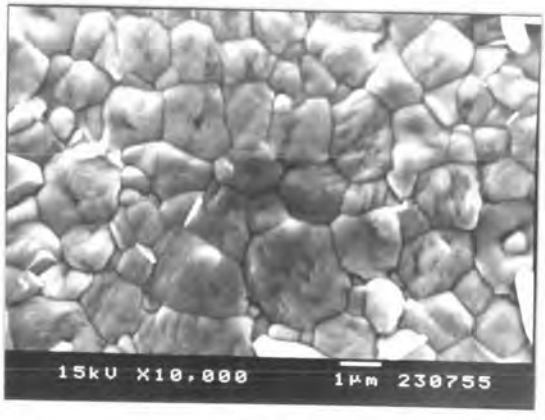

(c)

Fig.9 SEM photomicrographs of 0.95(0.90BNT-0.10PT)-0.05BaT at different sintering temperatures (a) 1150 °C (b) 1175 °C (c) 1200 °C

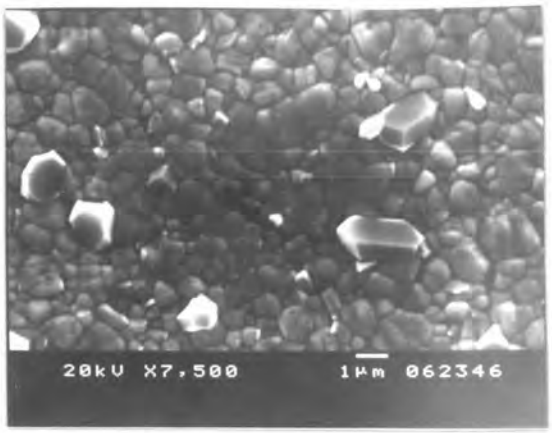

(a)

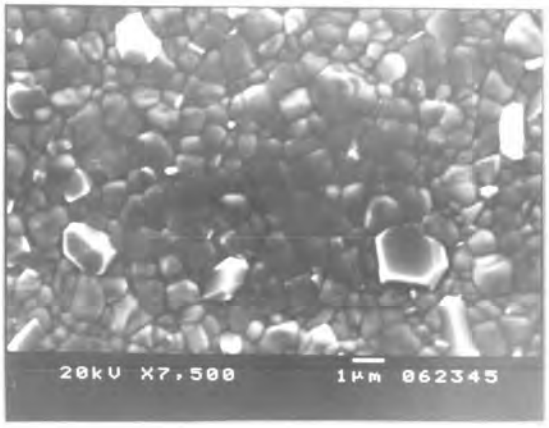

(b)

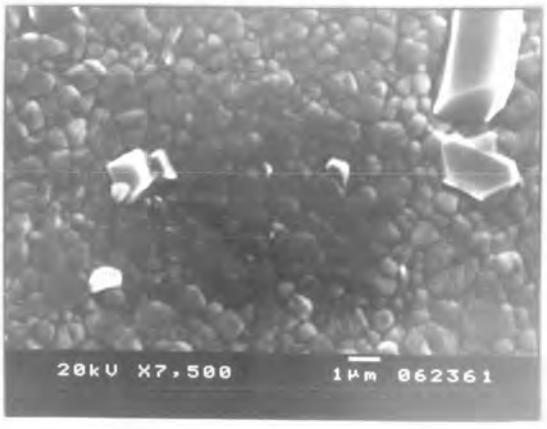

(c)

Fig.10 SEM photomicrographs of (1−x)BNT−xBaT at 1150 °C

(a) x = 0.05 (b) x = 0.10 (c) x = 0.15

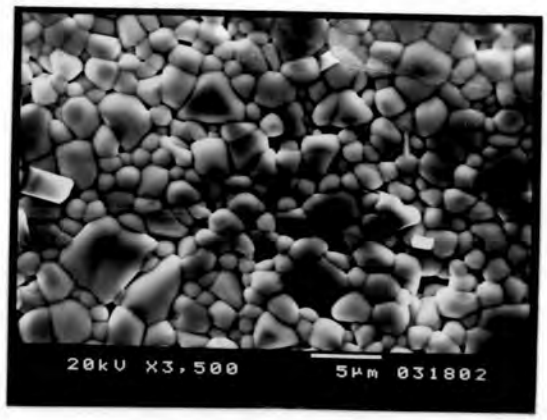

(a)

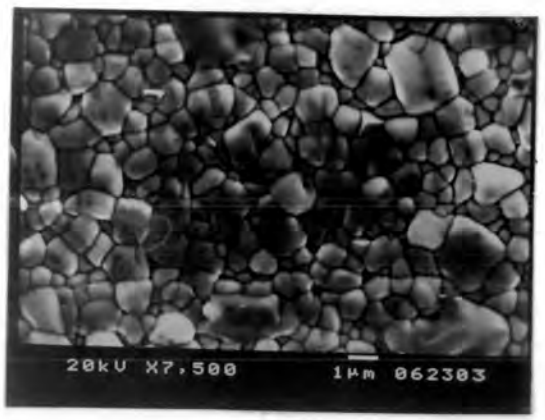

(b)

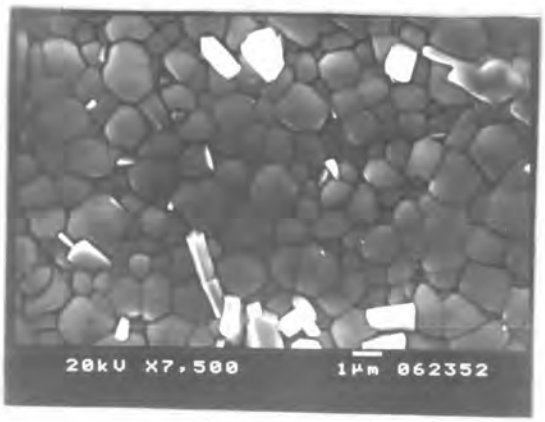

(c)

(d)

Fig.11 SEM photomicrographs of (1−x)BNT−xBaT at 1175 °C

(a) x = 0.0 (b) x = 0.05 (c) x = 0.10 (d) x = 0.15

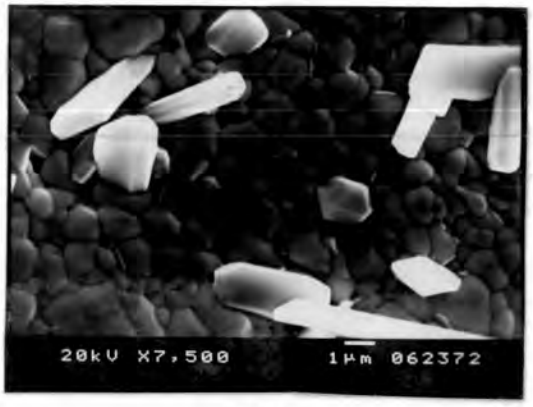

(a)

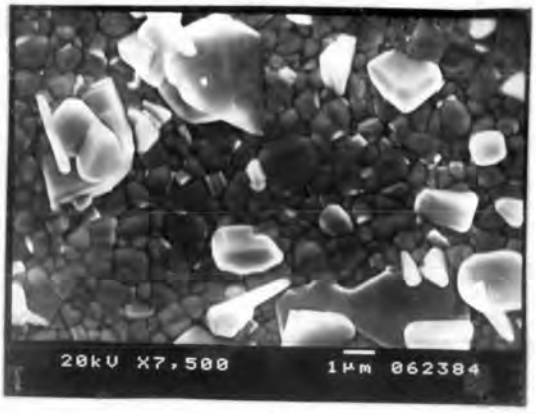

(b)

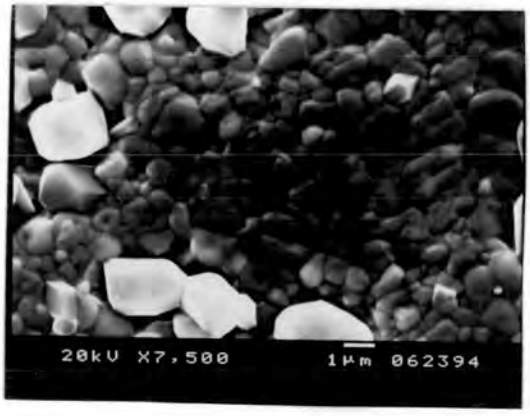

(c)

Fig.12 SEM photomicrographs of (1-x)[0.90BNT-0.10PT]-xBaT at 1150 °C
(a) x = 0.05 (b) x = 0.10 (c) x = 0.15

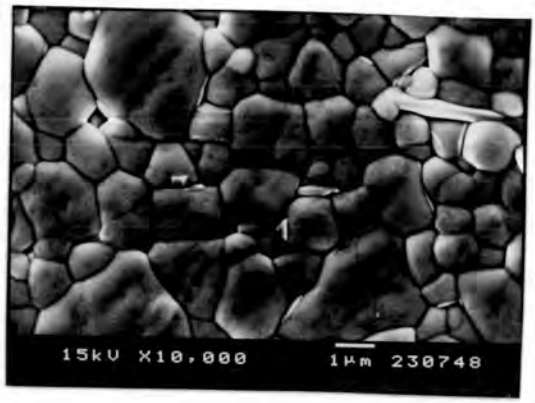

(a)

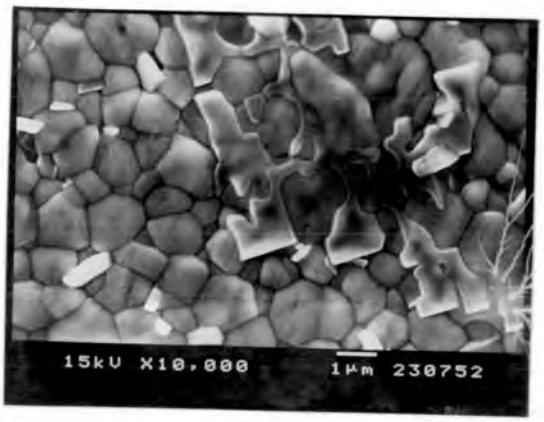

(b)

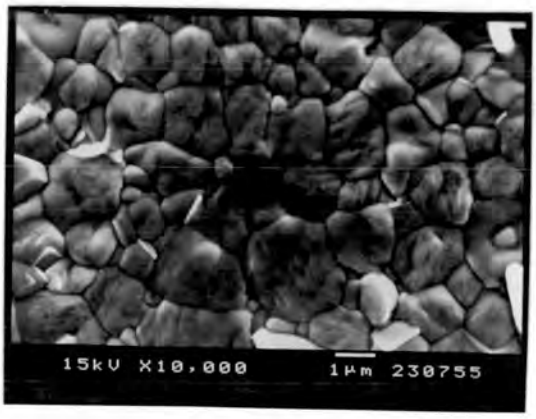

(c)

Fig.13 SEM photomicrographs of (1-x)[0.90BNT-0.10PT]-xBaT at 1175 ^{o}C

(a) x = 0.05 (b) x = 0.10 (c) x = 0.15

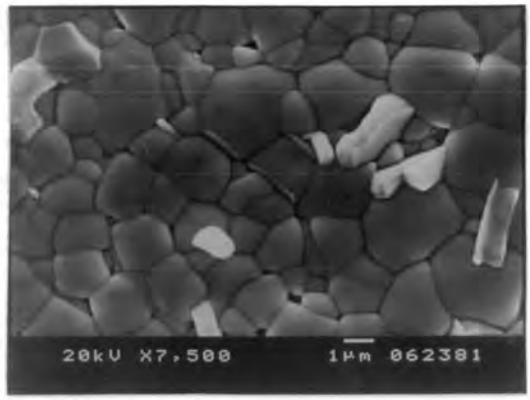

(a)

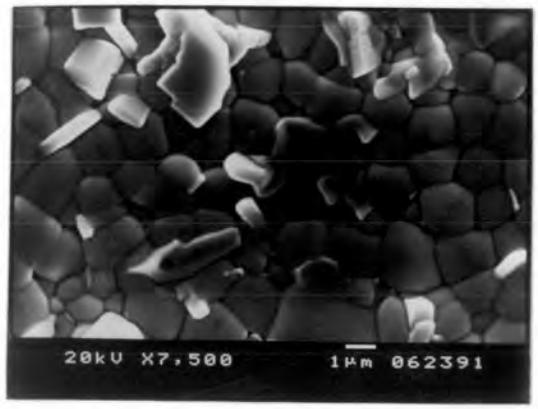

(b)

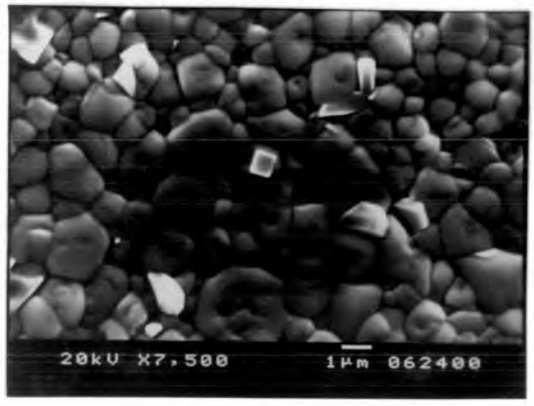

(c)

Fig.14 SEM photomicrographs of (1−x)[0.90BNT−0.10PT]−xBaT at 1200 °C
(a) x = 0.05 (b) x = 0.10 (c) x = 0.15

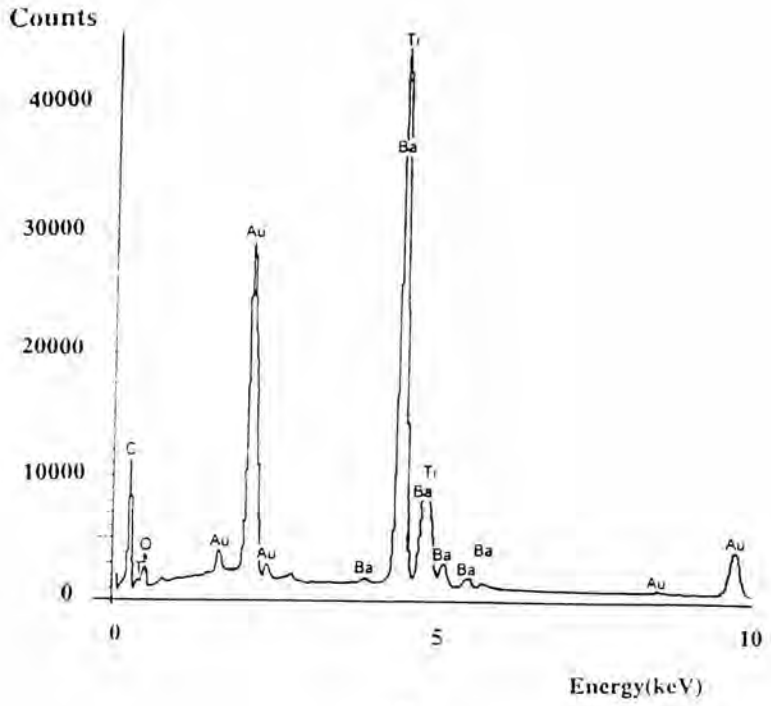

(a)

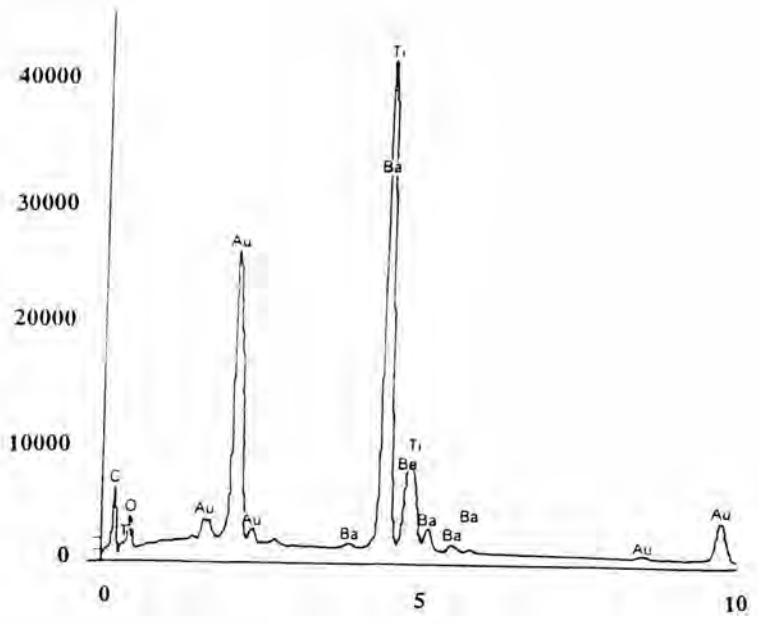

(b)

Fig.15 EDS analysis of 0.85BNT-0.15BaT second phases in different shapes
(a) circular shape (b) plate-like shape

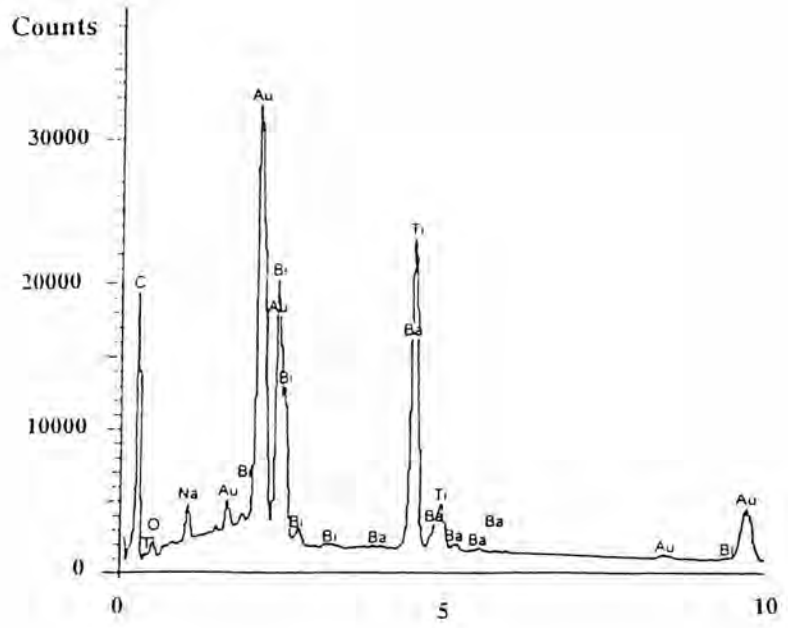

Fig.16 EDS analysis of single grain in 0.85BNT-0.15BaT

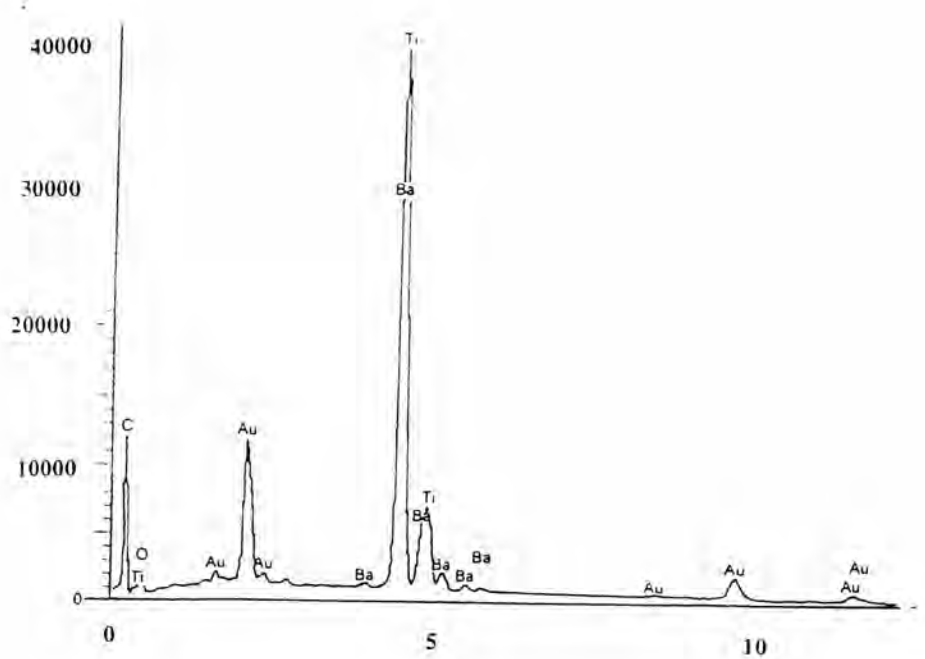

Fig.17 EDS anlysis of 0.90[0.90BNT-0.10PT]-0.10BaT second phase

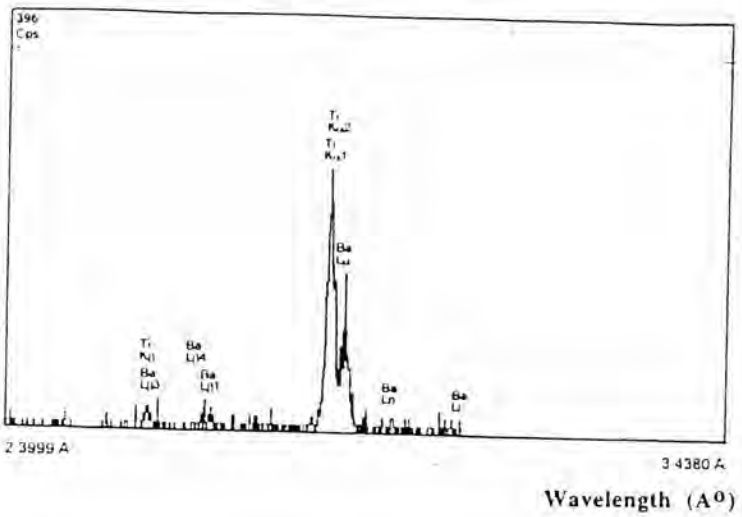

Fig. 18. WDS analysis of overlapping peak of Ba and Ti peaks